Combining evidence from human genetic and functional screens to identify pathways altering obesity and fat distribution
Supplementary materials

Nikolas A. Baya[1,2,*], Ilknur Sur Erdem[3,4*], Samvida S. Venkatesh[1,2], Saskia Reibe[1,5], Philip D. Charles[1], Elena Navarro-Guerrero[6], Barney Hill[1,5], Frederik Heymann Lassen[1,2], Melina Claussnitzer[7-10], Duncan S. Palmer[1,5,7,#], Cecilia M. Lindgren[1,2,3,7,#]

1. Big Data Institute, Li Ka Shing Centre for Health Information and Discovery, University of Oxford, Oxford OX3 7LF, United Kingdom.
2. Centre for Human Genetics, Nuffield Department of Medicine, University of Oxford, Oxford OX3 7BN, United Kingdom.
3. Nuffield Department of Women's and Reproductive Health, Medical Sciences Division, University of Oxford, United Kingdom.
4. Chinese Academy for Medical Sciences Oxford Institute, Nuffield Department of Medicine, University of Oxford, Oxford OX3 7FZ, United Kingdom.
5. Nuffield Department of Population Health, Medical Sciences Division, University of Oxford, Oxford, United Kingdom.
6. Target Discovery Institute, Nuffield Department of Medicine, University of Oxford, Oxford OX3 7FZ, United Kingdom.
7. Broad Institute of MIT and Harvard, Cambridge, Massachusetts, United States of America.
8. Broad Institute of MIT and Harvard, Novo Nordisk Foundation Center for Genomic Mechanisms of Disease & Type 2 Diabetes Systems Genomics Initiative, Cambridge, Massachusetts, United States of America.
9. Center for Genomic Medicine and Endocrine Division, Massachusetts General Hospital, Boston, Massachusetts, United States of America.
10. Harvard Medical School, Harvard University, Boston, Massachusetts, United States of America.

*, # shared authorship

Supplementary notes

Note S1. Calculating unweighted burden effect sizes

First, summary statistics for variant-level results are recalculated relative to the minor allele: the sign of the *t*-statistic is flipped if the original effect allele is not the minor allele and the frequency of the effect allele is recalculated accordingly. Then, for all single-variant and grouped ultra-rare variant burden results in a given gene which satisfy the maximum minor allele frequency and variant consequence of the desired result to unweight, the following summary statistics are summed: *t*-statistic, variance of *t*-statistic, and minor allele frequency. The unweighted *t*-statistic is calculated by dividing the summed *t*-statistics by the summed variance of *t*-statistics. The unweighted minor allele frequency is the summed minor allele frequency.

$$t_{unweighted,\,gene} = \frac{\sum_j t_{weighted,\,j}}{\sum_j Var(t_{weighted,\,j})}$$

$$MAF_{unweighted,\,gene} = \sum_j MAF_{weighted,\,j}$$

Note S2. Significant genes with low minor allele count

In sex-combined and sex differential gene-level associations we sought to avoid spurious associations by excluding putatively significant genes if they were supported by a total minor allele count (MAC) <5 across both sexes.

Among the sex-combined gene-level associations which were significant at FDR≤1% (SKAT-O $P \leq 4.37 \times 10^{-5}$), there were five genes which were excluded for having MAC<5: *DEFB112* (MAC=1), *CHMP4B* (MAC=2), *FEZF2* (MAC=3), *GLP1R* (MAC=3), and *PCBD2* (MAC=4) (Supp. Table 4).

In the sex differential analysis, we excluded a significant (sex-difference $P < 2.67 \times 10^{-6}$) differential effect at *SENP5* for visceral adipose tissue volume (female beta=0.08930 (0.028055), male beta=-0.09967 (0.028675), sex-difference $P = 2.33 \times 10^{-6}$) due to MAC<5 (female MAC=2, male MAC=2).

Note S3. Effect of *INSR* KO by pooling replicates

Although the *INSR* KO did not have significantly decreased glucose uptake in the insulin-stimulated state, as might be expected from the insulin receptor gene, we suspect that this may be due to small sample sizes when testing within basal/stimulated conditions, leading to weak statistical power to detect the effect. To check this, we pool together replicates from basal and insulin-stimulated states, which doubles the sample size of the test from six to 12, and jointly model effects of KO and insulin stimulus on glucose uptake with the following linear model:

glucose ~ is_ko + is_stimulated +1

We observe a significant effect of the *INSR* KO on glucose uptake (effect of KO in joint model=-0.22, two-sided *P*=0.0393). This effect was weaker in magnitude and statistical strength than those observed for gene KOs with significant effect on basal or insulin-stimulated glucose uptake (*PPARG* effect of KO in joint model=-0.48, $P=8.49 \times 10^{-4}$; *IRS2* effect=-0.46, $P=1.07 \times 10^{-3}$; *IRS1* effect=-0.41, $P=2.08 \times 10^{-3}$; *TBC1D4* effect=-0.28, $P=2.02 \times 10^{-2}$).

Supplementary tables

Table S1. Sample removal based on sample outliers defined by MAD thresholds (median ± 4 MADs), split by sequencing tranche.

QC Metric	# Samples in UK Biobank Whole Exome Sequencing Tranche		
	250k	**150k**	**50k**
Total before QC	**237,091**	**139,745**	**46,034**
Number of deletions	1,510	825	344
Number of insertions	1573	1,118	236
Number of SNPs	1,856	1,013	362
Ratio of insertions to deletions	1,741	954	339
Ratio of transitions to transversions	2,890	1,598	1781
Ratio of heterozygous variants to homozygous alternate variants	2,301	1,496	478
Total failing	10,861	6,396	3,238
Total passed QC	**226,230**	**133,349**	**42,796**
Grand total			**402,375**

For Supplementary Tables 2-15, refer to Excel file.

Table S2. Sample sizes for each obesity-related trait (sex-stratified and sex-combined)
Table S3. Variant-level results for significant variants (phenotype, variant, gene, beta & SE, p-value)
Table S4. Gene-level results for all FDR≤1% significant genes
Table S5. Phenome-wide associations from Genebass
Table S6. Gene-level results for genes that only reach significance in sex-specific strata and genes with significant heterogeneity in effect sizes between sexes (phenotype, male-specific beta & SE & P, female-specific beta & SE & P, sex-heterogeneity P-value)

Table S7. Obesity age-of-onset longitudinal analysis using Cox proportional hazards model
Table S8. Proteins associated with obesity (only significant results) with protein, phenotype, beta, SE, P
Table S9. Pathway analysis for proteins that are associated with obesity (all significantly upregulated and all significantly downregulated)
Table S10. Obesity-gene burden effect on proteome (only [exome-wide] significant results) with gene, protein, beta, SE, P
Table S11. Combined evidence table (hWAT counts, literature review)
Table S12. Guide RNAs per gene target
Table S13. Effect of KO on lipid and glucose assays
Table S14. Genes differentially expressed between each knockout and Cas9-empty, with logFC and P-value
Table S15. GSEA pathway analysis for RNA-seq of KOs

Supplementary figures

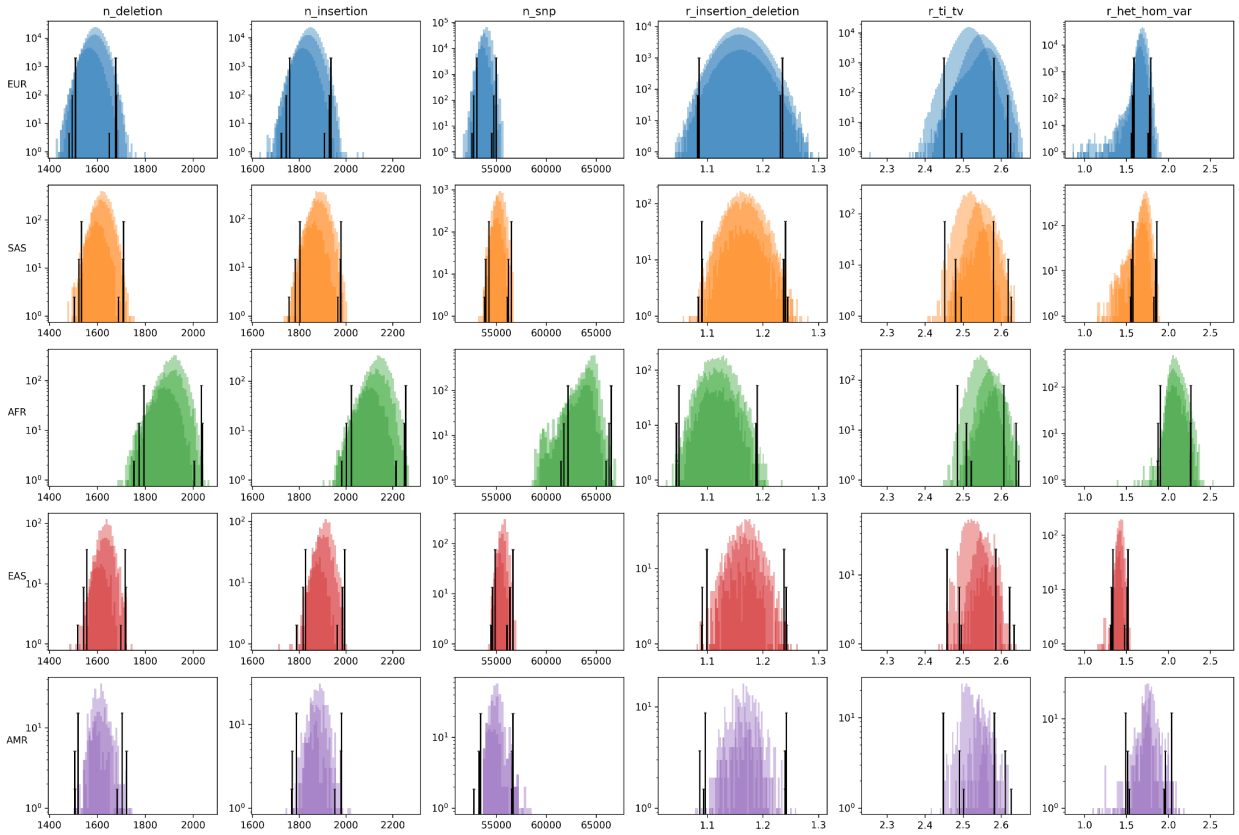

Figure S1. MAD thresholds, split by tranche. Samples with any of n_deletion, n_insertion, n_snp, r_insertion_deletion, r_ti_tv, and r_het_hom_var exceeding four MADs from the median are removed. MAD thresholds are displayed as vertical lines, conditional on tranche size (50k, 200k, 250k).

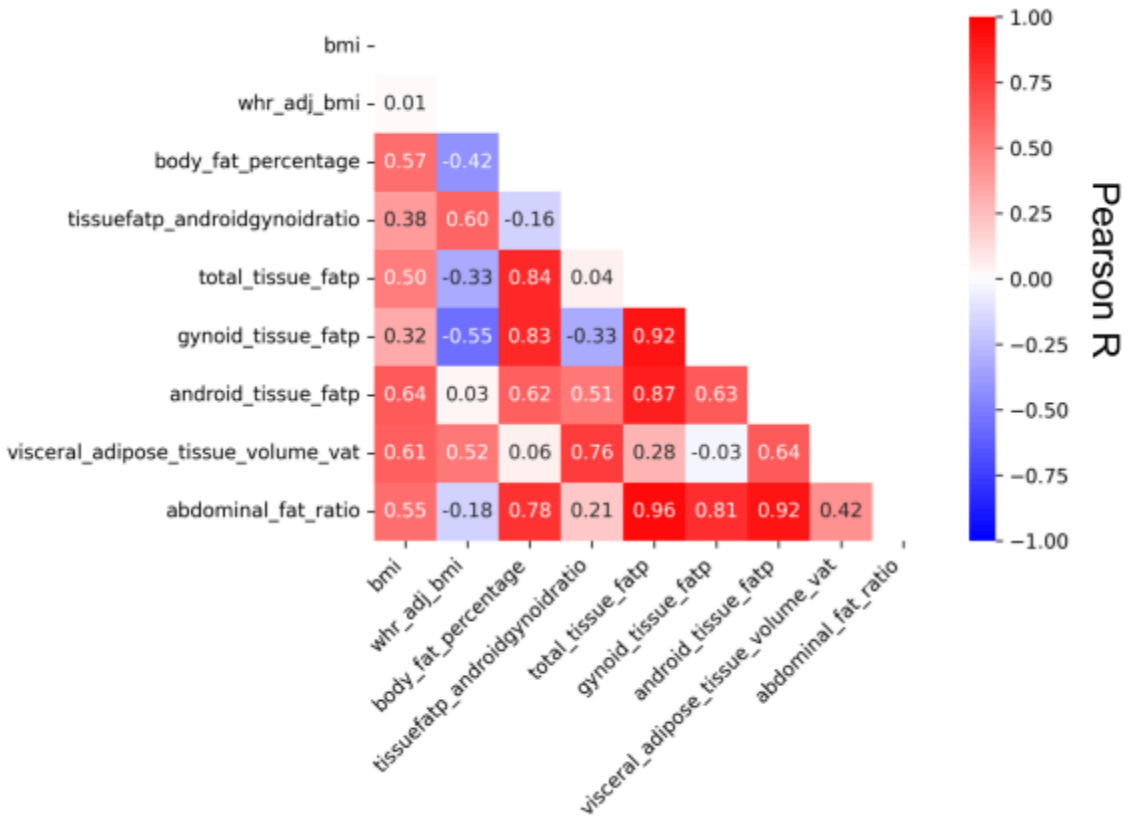

Figure S2. Obesity and fat distribtuion trait correlation heatmap. Correlations for this heatmap were calculated using the subset of individuals used for our genetic association testing. By definition of WHRadjBMI, correlation between BMI and WHRadjBMI should be zero, but here it is nonzero (R=0.01) because WHRadjBMI was calculated on a superset of individuals used for the correlations.

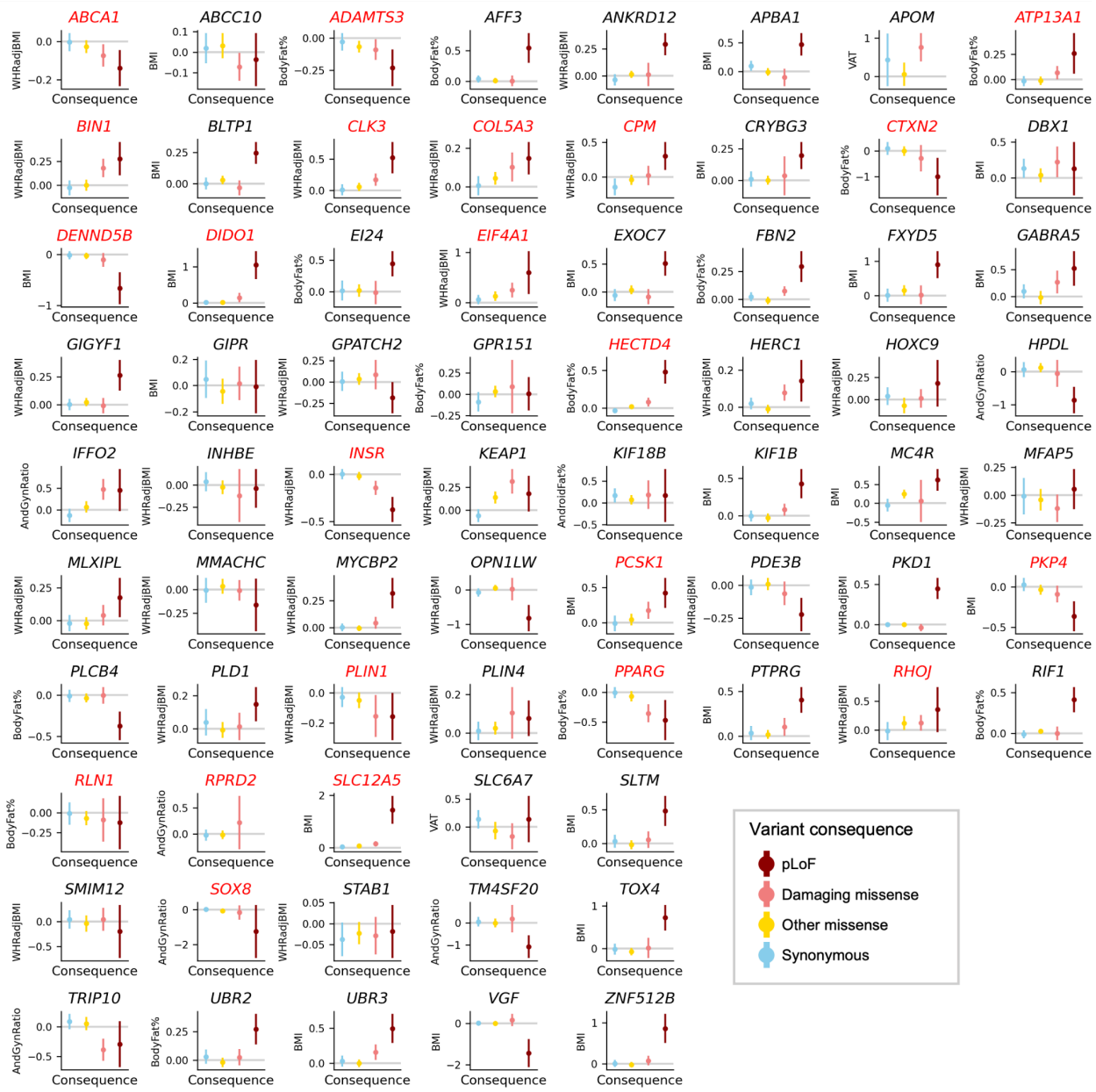

Figure S3. Ultra-rare variant allelic series for all FDR≤1% significant genes. Monotonic allelic series are highlighted with red gene symbols. Allelic series are defined as monotonic if they have strictly increasing or strictly decreasing effect sizes across increasingly deleterious variant consequences (least to most deleterious: synonymous, other missense, damaging missense, pLoF). Effect sizes come from ultra-rare variant burden for variants with minor allele count≤10 in each gene, grouped by variant consequence. Confidence intervals for effect size defined as +/-1.96 standard errors. pLoF, predicted loss-of-function.

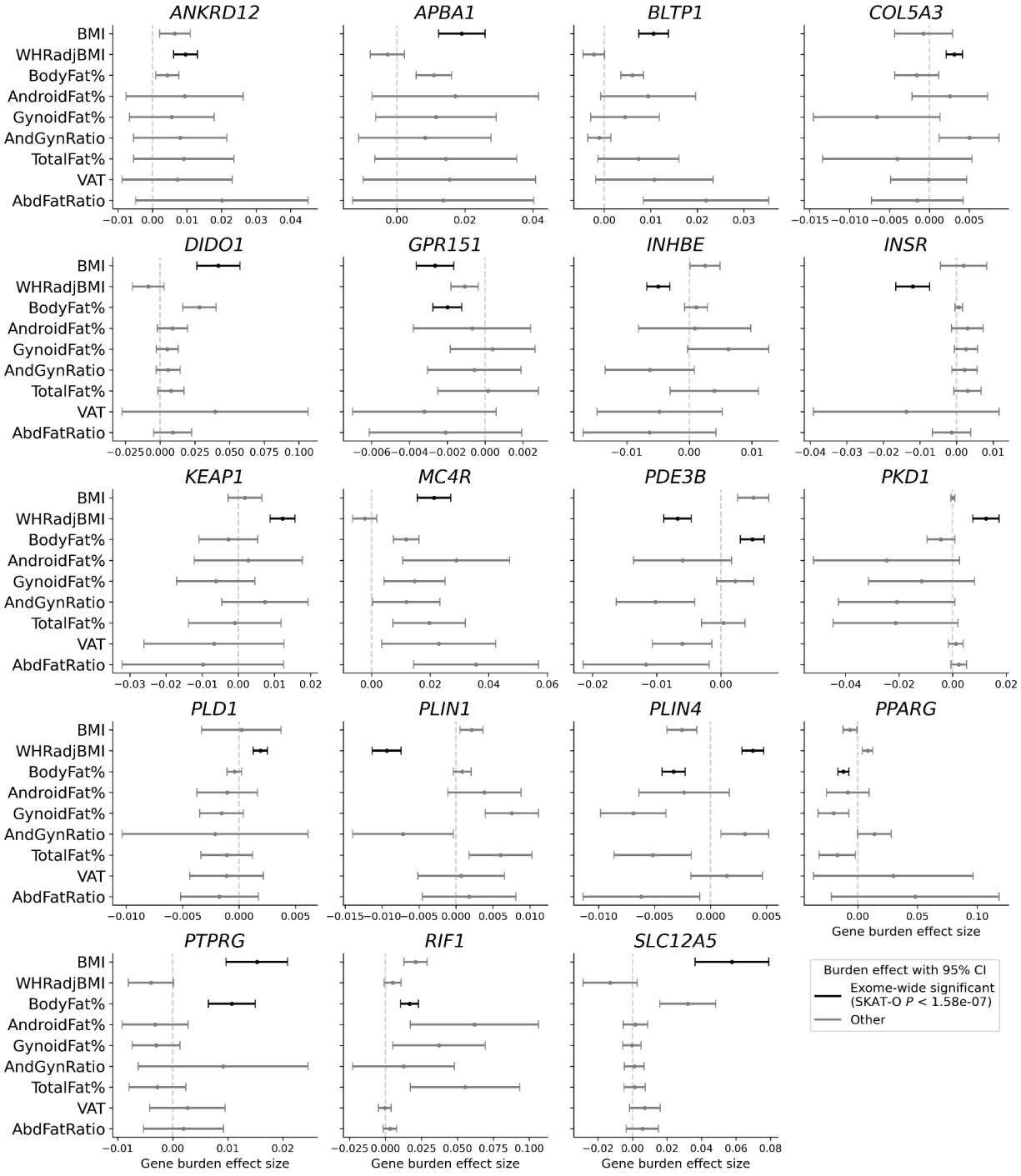

Figure S4. Gene burden effects across all nine obesity and fat distribution traits for 19 genes with exome-wide significant burden associations. Confidence intervals for effect size defined as +/-1.96 standard errors. Only the result of the consequence mask with the lowest SKAT-O *P* is shown for each trait-gene pair. The vertical dotted line marks an effect size of zero.

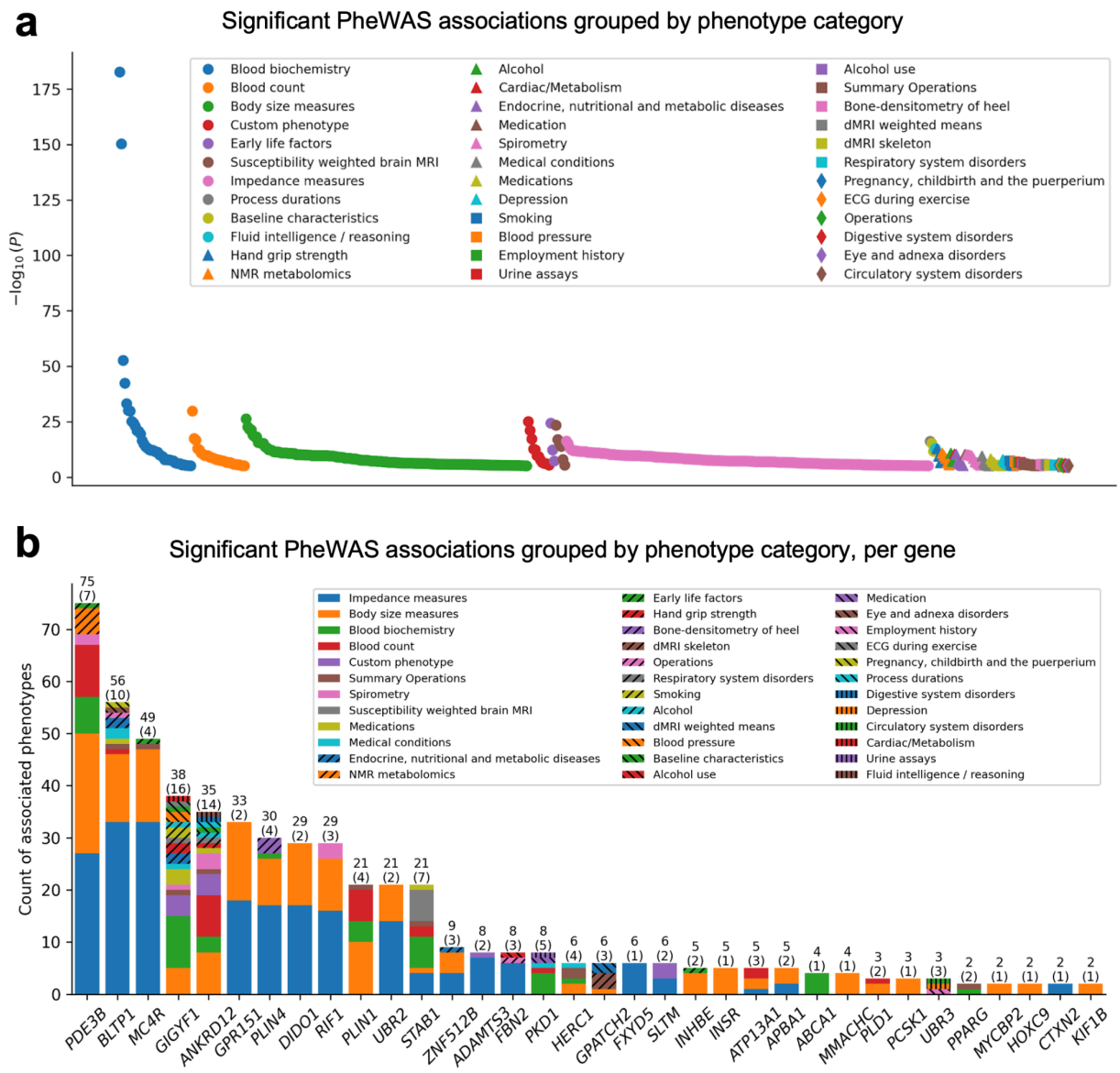

Figure S5. PheWAS of obesity and fat distribution associated genes using Genebass summary statistics. Only the pLoF variant mask results from Genebass are used. Significant associations are controlled for FDR≤1% (SKAT-O P≤9.69×10^{-6}), resulting in 549 significant associations across 211 phenotypes and 42/71 obesity and fat distribution associated genes. **a,** Significant associations grouped by phenotype category, with phenotype groups ordered from left to right by the lowest P-value in the category. Significance of association is measured on the y-axis as -log$_{10}$(Genebass SKAT-O P-value). **b,** Significant associations per gene, grouped by phenotype category. The total number of significant phenotype associations is shown at the top of each bar, with the number of phenotype categories shown in parentheses. Only genes with at least two phenotype associations are shown.

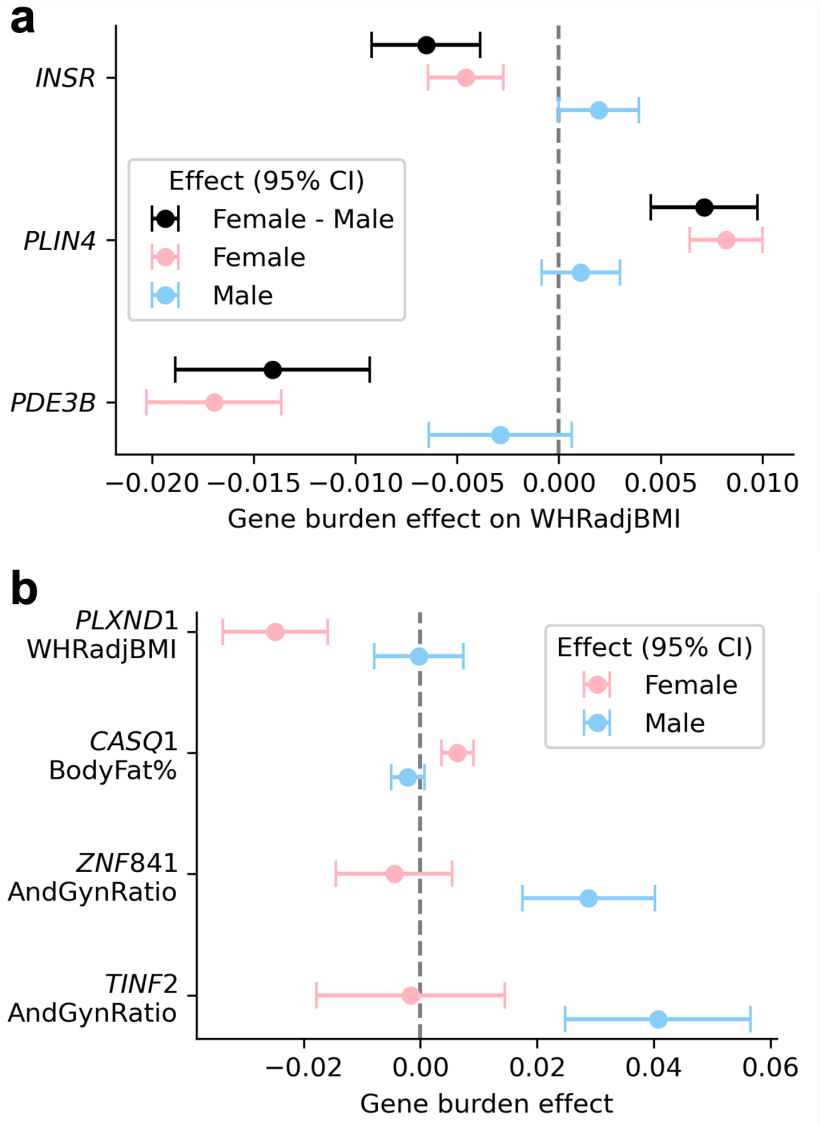

Figure S6. Sex-differential and sex-specific analysis. a, Genes with significant sex-differential effects (sex-difference $P<2.67\times10^{-6}$, Bonferroni adjusted for 18,737 genes tested for sex-differential effects). All three significant sex-differential gene burden effects are on WHRadjBMI. **b,** Female- (*PLXND1, CASQ1*) and male-specific (*ZNF841, TINF2*) gene-level significant associations ($P<2.67\times10^{-6}$, Bonferroni adjusted for 18,737 genes tested for sex-specific effects). Confidence intervals for effect size defined as +/-1.96 standard errors.

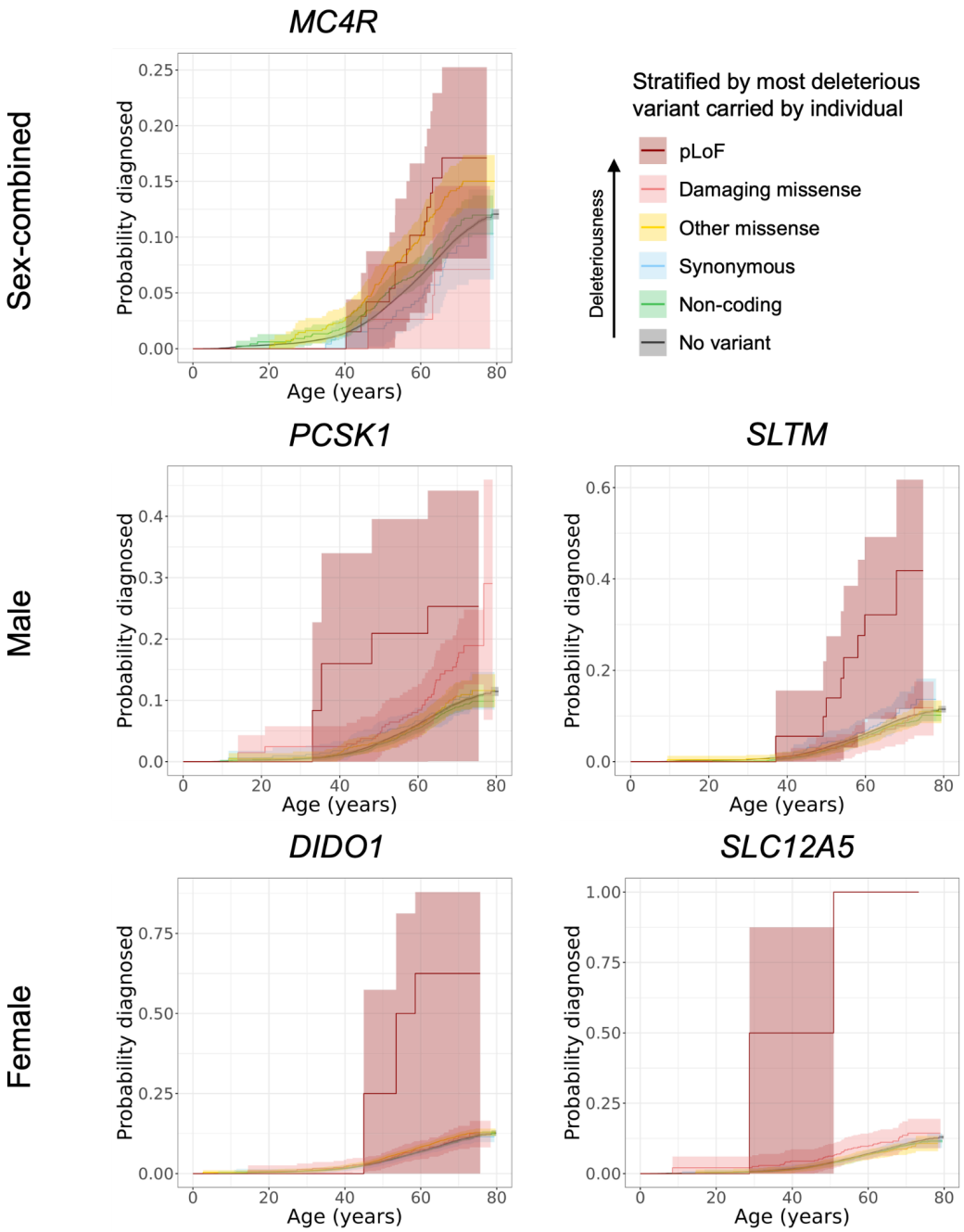

Figure S7. Longitudinal obesity age-at-onset analysis. Longitudinal analysis was performed using Cox-proportional hazards modelling (Methods). Individuals are stratified by the most deleterious carried in the gene. Only genes with significant age-of-onset associations in both sexes (*MC4R*), males only (*PCSK1, SLTM*), or females only (*DIDO1, SLC12A5*) are shown. 95% confidence intervals are indicated by shading.

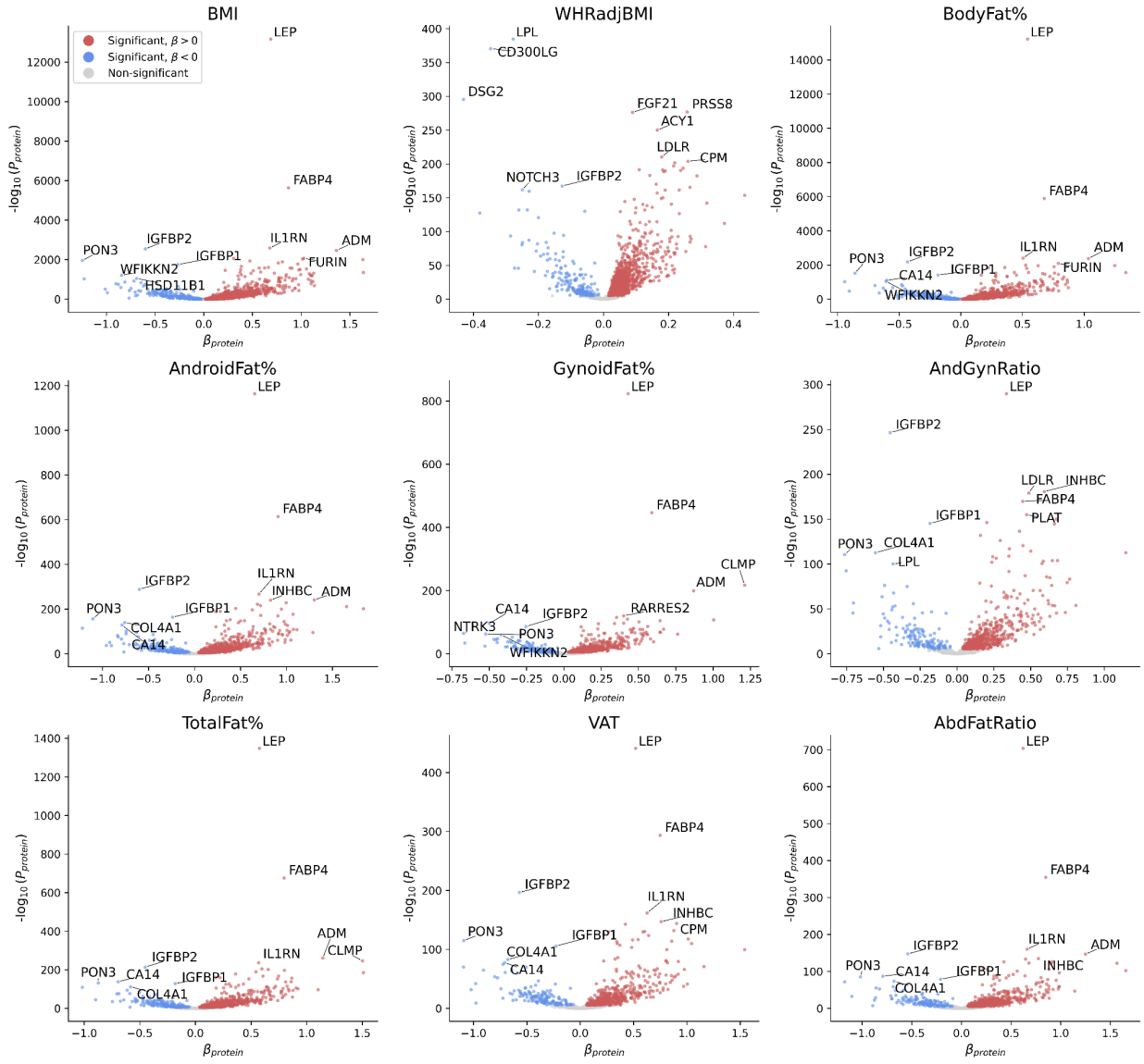

Figure S8. Beta vs p-value plots (volcano) for proteins on all nine obesity and fat distribution phenotypes in separate panels. Top five most significant positive and negative associations are labeled. Red and blue points are protein associations with $P<3.80\times10^{-6}$ and positive or negative effect on the trait, respectively. Grey points are associations which do not reach statistical significance.

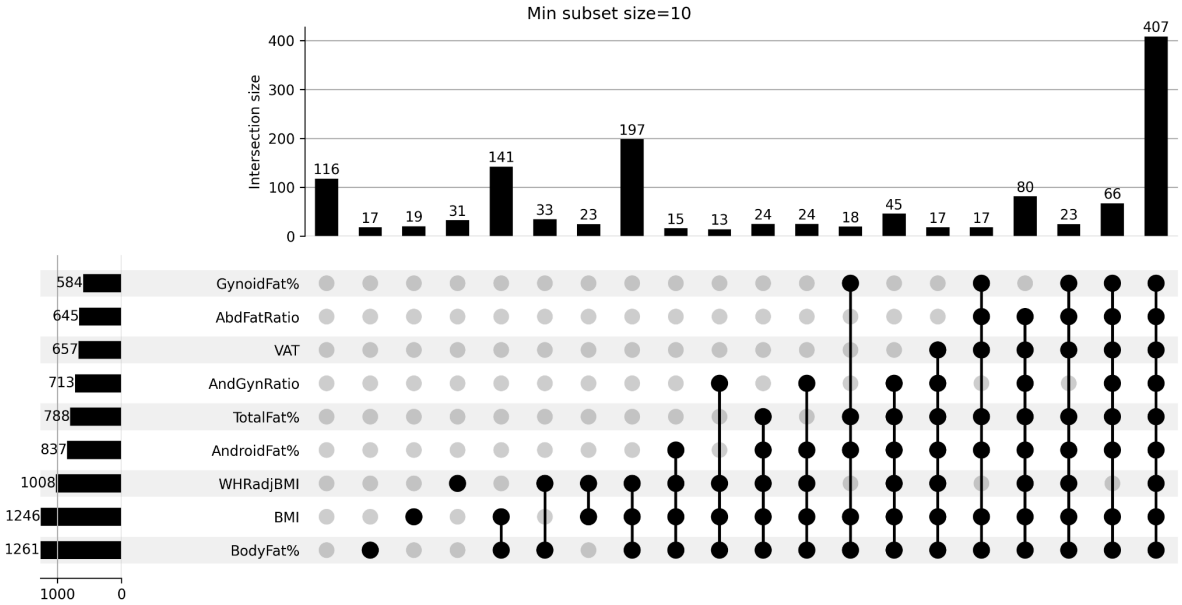

Figure S9. UpSet plot with number of proteins associated with each obesity or fat distribution phenotype. Only subsets with 10 or more significant associations (P<3.80×10^{-6}) are shown. Plot was generated with the Python package UpSetPlot (Methods).

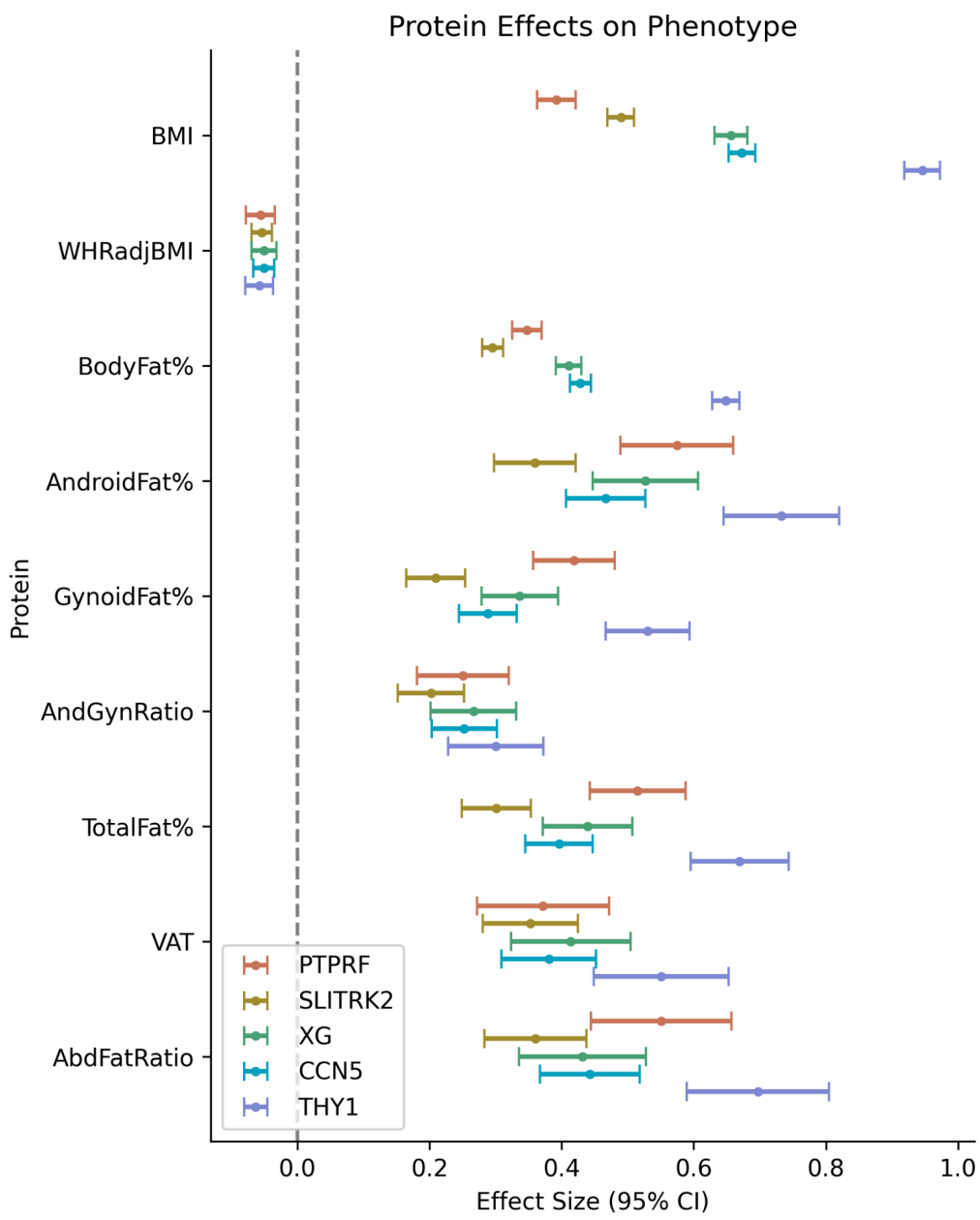

Figure S10. Forest plots for the five proteins with differential effects on obesity and fat distribution traits. Selected proteins are significantly associated with all obesity and fat distribution traits, with a negative effect on WHRadjBMI and positive effects on all other traits in the study. Confidence intervals for effect size defined as +/-1.96 standard errors.

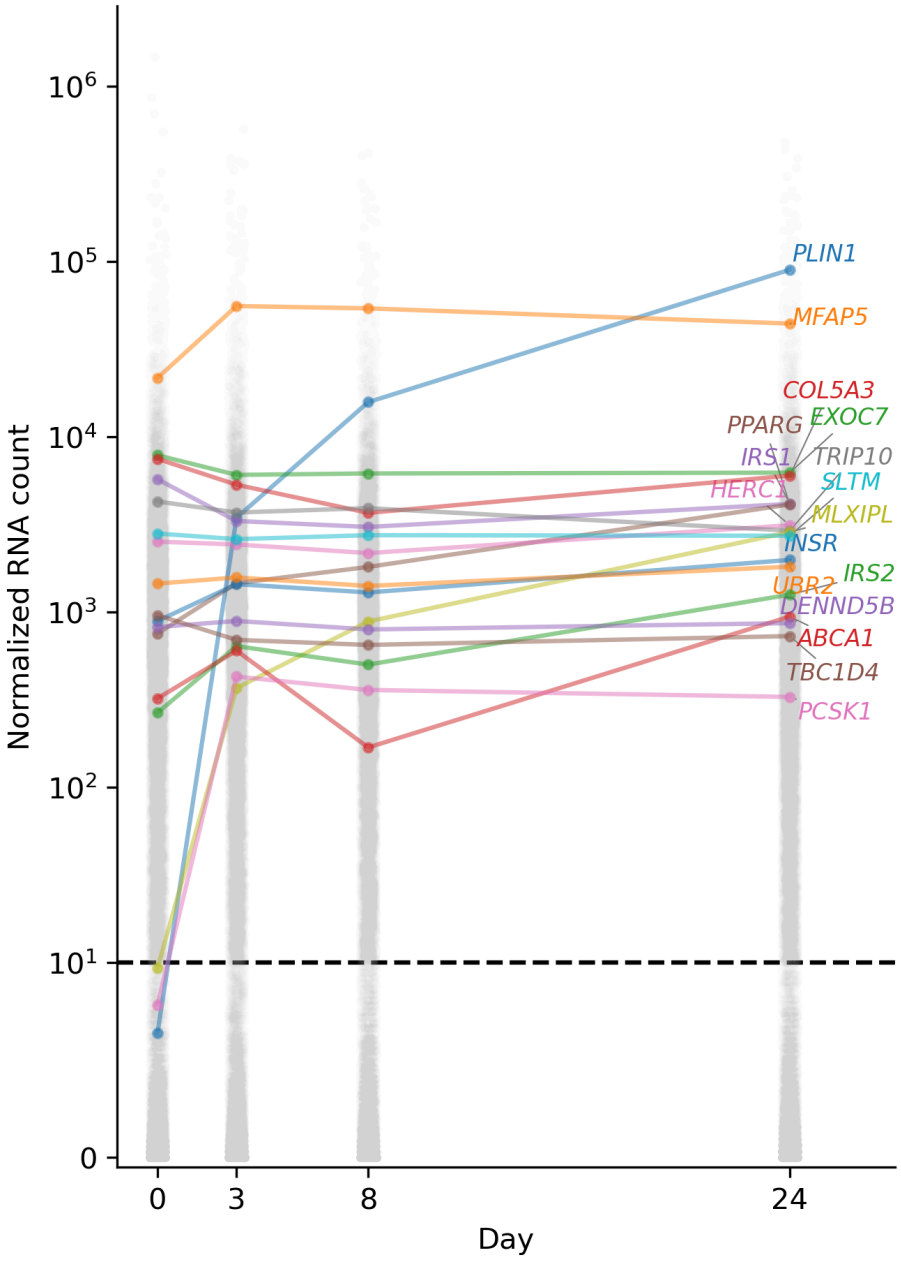

Figure S11. Longitudinal mRNA expression in wild type human white adipose tissue of genes selected for KO. Normalized mRNA count was measured at four time points across 24 days of differentiation. Day 0 corresponds to the undifferentiated state. Colored traces are genes selected for KO. All other genes are indicated with grey points. The horizontal dashed line indicates the minimum threshold needed on days 8 and 24 for a gene to be selected as a KO. The y-axis uses the 'symlog' scale, such that the scale is linear between 0 and 10 and logarithmic for values greater than 10.

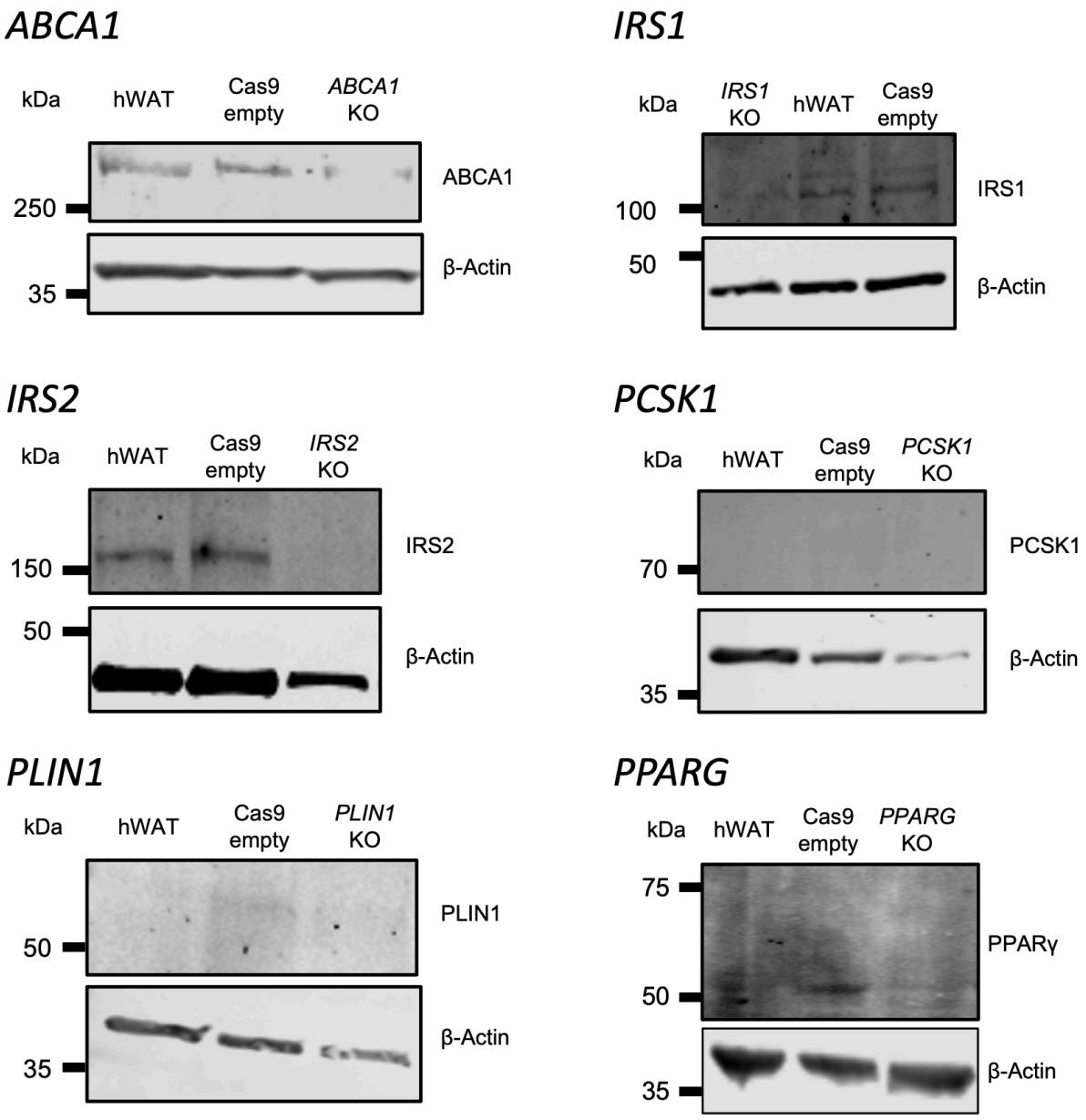

Figure S12. Western blots for confirmation of KO. Western blots were performed using undifferentiated adipocytes. Only genes which could not be confirmed by mRNA expression were included for confirmation by western blot.

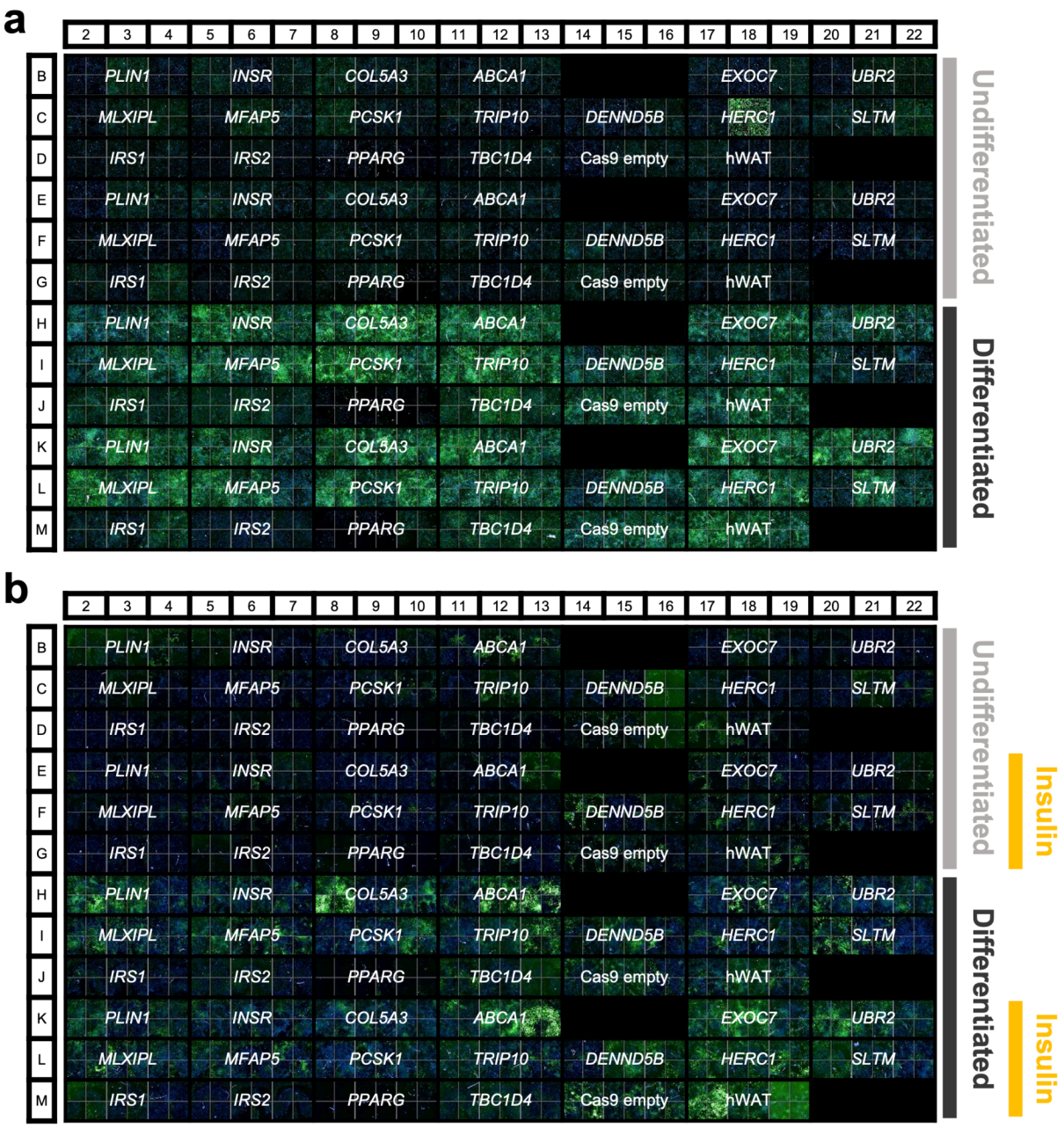

Figure S13. Imaging of well plates for lipid accumulation and glucose uptake assays of KO adipocytes. (A) Lipid accumulation is highlighted in green by fluorescent BODIPY staining. Each KO has six replicates for each differentiation status (undifferentiated, differentiated). (B) Glucose uptake is highlighted in green by fluorescent 2-NBDG glucose analog. Each KO has six replicates for each differentiation status (undifferentiated, differentiated), which are further split into three replicates for each stimulus condition (basal/unstimulated, insulin stimulus).